



The status of $p\bar{p}$ collider physics ¹

R. K. Ellis

*Fermi National Accelerator Laboratory
P.O. Box 500, Batavia, Illinois 60510, U.S.A.*

Abstract

A summary of the current status of $p\bar{p}$ physics is given.

¹Summary talk at the 8th topical workshop on proton antiproton collider physics, Castiglione della Pescaia, September 1989.



1. Heavy quark production

1.1 Limits on the masses of new heavy quarks.

The ability to set limits on the mass of the top quark in $p\bar{p}$ collisions depends crucially on our understanding of the production cross section. In the Born approximation there are three partonic mechanisms by which a top quark may be produced at a hadronic collider.

$$\begin{aligned}
 1) \quad q\bar{q} &\rightarrow t\bar{t} + X \\
 2) \quad gg &\rightarrow t\bar{t} + X \\
 3) \quad q\bar{q} &\rightarrow W + X \\
 &\quad \quad \quad \downarrow \\
 &\quad \quad \quad t + \bar{b}.
 \end{aligned}
 \tag{1.1}$$

Process three is viable as a source of top quarks only if the decay $W \rightarrow t\bar{b}$ can occur. The importance of the third process can be fixed experimentally from the observed rate for $W \rightarrow e\nu$, assuming the branching ratios of the standard model. The rates for the first two processes are controlled by the parton cross-sections which have been calculated through order α_S^3 [1] and by the flux of quarks and gluons which are energetic enough to produce a pair of heavy quarks of a given mass. At $\sqrt{S} = 0.63$ TeV, the continuum production of top quarks with mass heavier than about 40 GeV is dominated by quark-antiquark annihilation. At $\sqrt{S} = 1.8$ TeV the quark-antiquark process only dominates for $m_t > 100$ GeV. The total cross section[1,2] is shown as a function of top quark mass in Fig. 1. The band of values gives an estimate of the theoretical error due to uncertainties in α_S and in the structure functions. The scale at which the running coupling α_S and parton distributions are evaluated is denoted by μ . The μ dependence of the cross section gives some idea of the importance of uncalculated higher orders. As an example the μ dependence of the cross section for the production of a 120 GeV top quark is shown in Fig. 2. The inclusion of next-to-leading (NL) corrections reduces the μ dependence of the theoretical prediction. In the region in which the production is dominated by quark antiquark annihilation the theoretical error on the cross section is expected to about $\pm 25\%$. This error is estimated by varying the coupling constant α_S , the parton distributions and the scale μ in reasonable ranges.

Experiment	Limits [GeV] (95% Confidence level)	Signal
UA1[3]	$m_t > 53$	Single muon + 2 jets
UA1[3]	$m_{b'} > 41$	Single muon + 2 jets
UA1[4]	$m_t > 46$	Dimuon events
UA2[5]	$m_t > 67$	Electron + jets
UA2[5]	$m_{b'} > 53$	Electron + jets
CDF[6]	$40 < m_t < 77$	Electron + jets
CDF[7]	$28 < m_t < 72$	Electron + muon
KEK (Amy)[8]	$m_t > 30.4, m_{b'} > 29.8$	Isolated lepton
SLC(Mark II)[9]	$m_t > 38.5, m_{b'} > 43$	Event shape

Table 1: Limits on the masses of the top and b' quark

The experimental limits on the mass of the top quark are shown in Table 1. Note that most of these limits assume the standard branching ratio into leptons $BR(t \rightarrow l + X) = 11\%$. The highest limit is provided by the CDF electron plus jets analysis[6]. Approximately comparable limits are derived from analyses performed in different decay channels. In the troublesome region in which the mass of the top is within 20 GeV of the mass of the W , the cleanest analysis comes from the sample of events with an electron and a muon in the final state. In the CDF analysis candidate electron muon events are selected according to criteria detailed in ref.[7]. The resulting sample of 45 candidate events is shown in Fig. 3. The top signal region is defined as

$$p_T(\mu) > 15 \text{ GeV}, \quad E_T(e) > 15 \text{ GeV}, \quad (1.2)$$

so as to avoid the background, primarily due to bottom quarks. The expected signal in this region is 33(7.5) events for a top quark of mass 28(70) GeV. In the signal region one $e\mu$ event is expected from the process $Z^0 \rightarrow \tau\tau$ and 0.2 events from $Z^0 \rightarrow b\bar{b}$. Vector boson pair production gives 0.15 events from WW and 0.05 events from WZ in the signal region.

One event is found in the top signal region as shown in Fig. 3. This event has an isolated electron with $E_T = 31.7$ GeV and an isolated opposite sign muon with $p_T = 42.5$ GeV. This event also contains a second muon candidate in the forward muon detector with a transverse momentum of 10 GeV and a jet with a calorimeter

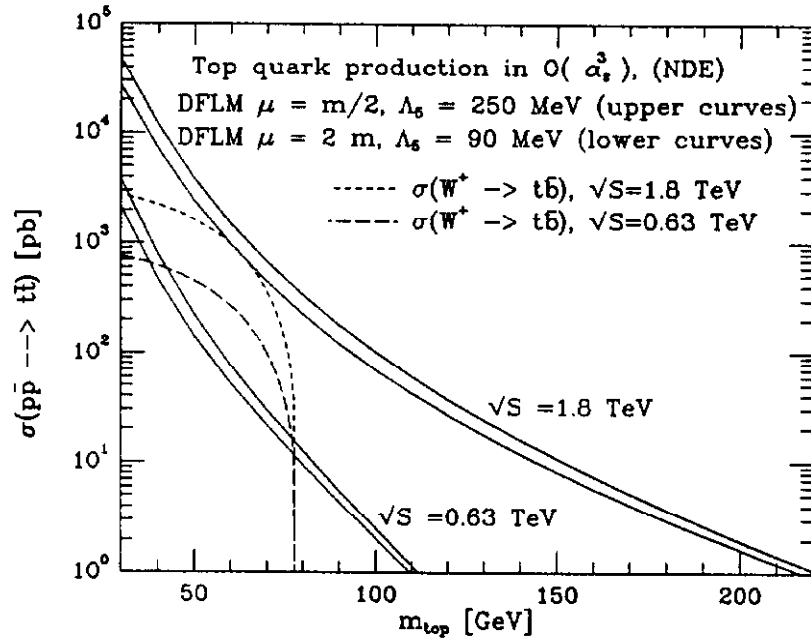


Figure 1: Cross-section for top quark production

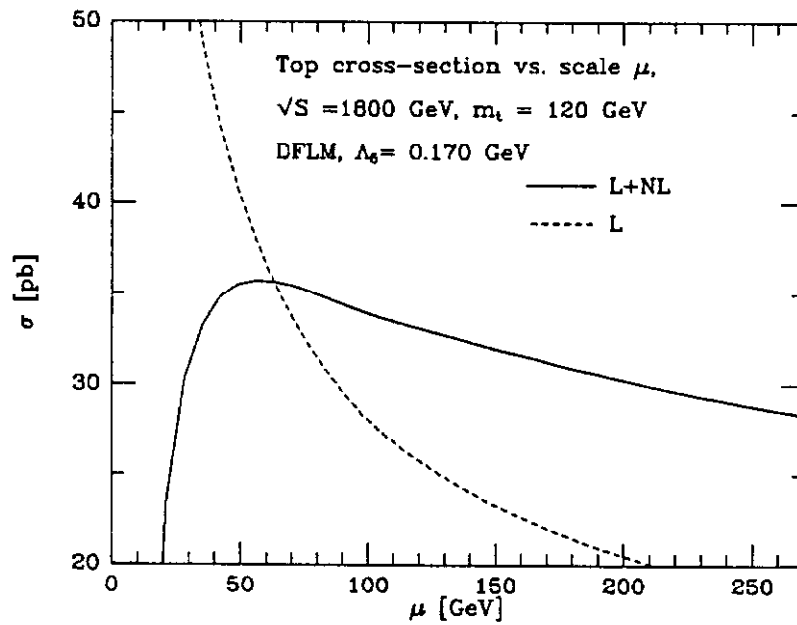


Figure 2: μ dependence of cross-section for top quark production

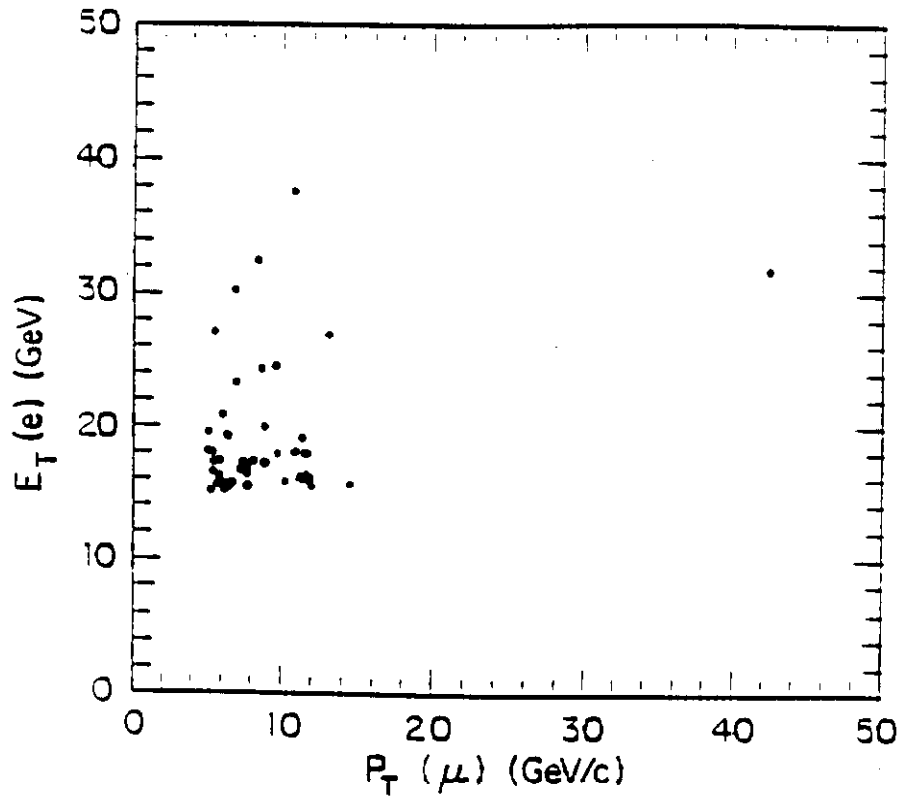


Figure 3: Electron transverse energy vs. muon transverse momentum in 4.4 inverse picobarns of CDF data.

transverse energy deposition of 14 GeV.

The conclusion from the results of this year is that the top quark is unlikely to be found in the decay products of the W . From Table 1 one can see that $m_t > m_W - m_b$ at 95% confidence level. It therefore appears that the top quark is rather special. It is more than 50 times heavier than the charm quark and more than 15 times heavier than its sibling, the bottom quark. Dynamical symmetry breaking schemes which link the mass of the top quark to the scale of electroweak symmetry breaking suggest top quark masses in excess of two hundred GeV[10]. The upper bound on the top quark mass from precision electroweak measurements is considered later in this report.

The above limits are derived under the assumption of standard branching ratio. A simple model which leads to a non-standard top quark decay is the two Higgs doublet model which has been investigated (*inter alia*) by Glashow and Jenkins[11]. Top limits can be translated into bounds on the ratio of the vacuum expectation values of the two Higgs fields[12].

1.2 Future prospects

The future prospects for the discovery of the top quark can be judged from Fig. 1. The elimination of the region $m_T < m_W - m_b$ appears to put the top quark out of reach of the CERN collider with the presently expected increase in the accumulated luminosity. I shall therefore concentrate on the discovery potential at the Tevatron. The next scheduled run of the Tevatron begins in June 1991, when an integrated luminosity of about $20pb^{-1}$ is expected to be recorded by both the CDF and the D0 detector. From Fig. 1 it might be assumed that an increase of the exposure by a factor of four would increase the top quark limit by only 20 GeV. The increase in reach is in fact considerably greater because, when $m_t \gg m_W$, the b jet present in the decay $t \rightarrow W + b$ is stiff enough to be resolved. The decay of the t and the \bar{t} produces W plus three or four resolved jets and the problem of QCD background, present in the W plus two jets channel is less severe.

1.3 Bottom quark production

Bottom quark production remains of great interest. It is vital to have good information on the cross-section for the production of bottom quarks to assess the feasibility of hadronic experiments dedicated to the study of bottom. Unfortunately, little new information on this subject was presented at this conference. The UA1 collaboration[13] presented a new result, shown in Fig. 4, from the analysis of $e\mu$ events using old data from the 1984-1985 run. The theoretical curves in Fig. 4 are from ref. [14]. The new experimental result is consistent with the published results[15] using other signatures for bottom quarks. Note that the problem of the excess of bottom quarks observed experimentally at large k^{min} is not yet understood.

The only other result on bottom quarks presented at this conference by the UA1 collaboration[16] is a confirmation of earlier results on $B^0 - \bar{B}^0$ mixing. Let $N(B^0)(N(\bar{B}^0))$ be the number of particles which decay as $B^0(\bar{B}^0)$ given an initially pure beam of B^0 mesons. We define χ as

$$\chi = \frac{N(\bar{B}^0)}{N(B^0) + N(\bar{B}^0)} \quad (1.3)$$

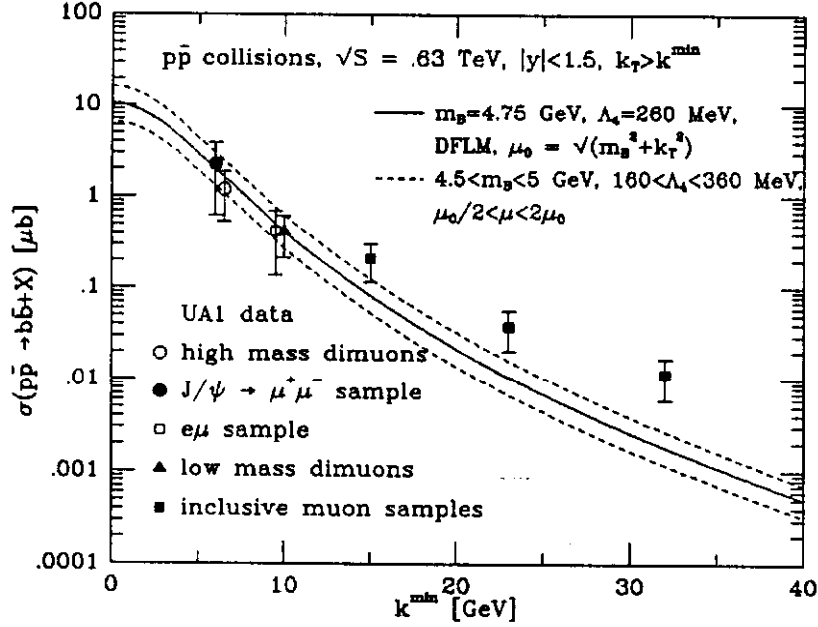


Figure 4: Cross-section for bottom quark production

UA1 find that,

$$\chi = 0.18 \pm 0.08, \quad 1989$$

$$\chi = 0.16 \pm 0.06, \quad 1983 - 1985. \quad (1.4)$$

In order to make statements about $B_d^0 - \bar{B}_d^0$ and $B_s^0 - \bar{B}_s^0$ mixing one must unfold to obtain χ_d and χ_s separately,

$$\chi = p_d \chi_d + p_s \chi_s, \quad p_i = h_i \frac{B(B_i^0 \rightarrow \mu)}{B(b \rightarrow \mu)} \quad (1.5)$$

This requires knowledge of h_i , the fraction of b quarks which hadronise as B_i^0 mesons, $B(B_i^0 \rightarrow \mu)$, the semi-muonic branching ratio of B_i^0 mesons and $B(b \rightarrow \mu)$, the average semi-muonic branching ratio for all bottom hadrons. In Fig. 5 the results are shown assuming $p_d = 0.36$, $p_s = 0.18$ for UA1 and $p_d = 0.45$, $p_s \approx 0$ for ARGUS and CLEO. UA1 conclude that both $B_d^0 - \bar{B}_d^0$ and $B_s^0 - \bar{B}_s^0$ mixing are needed to explain the data.

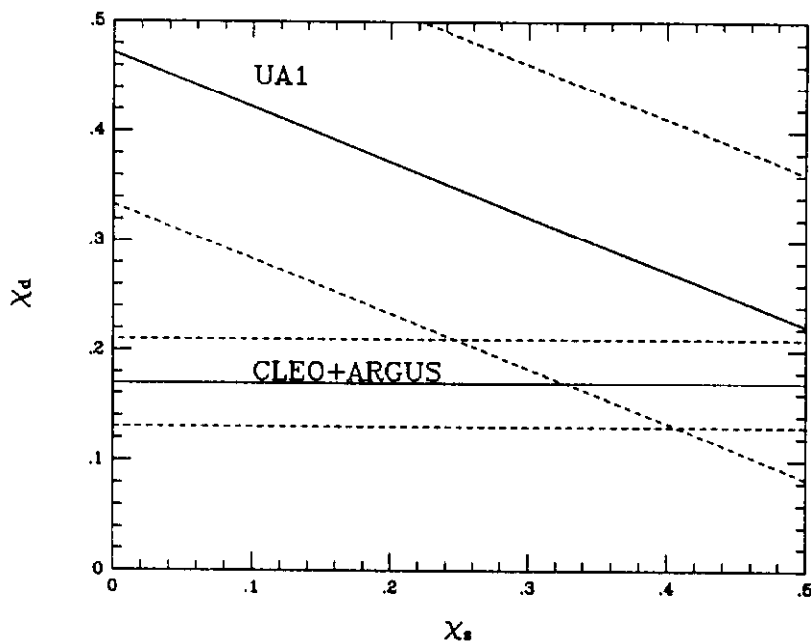


Figure 5: Mixing results from UA1 compared with CLEO and ARGUS

1.4 D-mesons in jets

A question of experimental interest is the frequency with which heavy quarks are found amongst the decay products of a jet. Since hadrons containing heavy quarks have appreciable semi-leptonic branching ratios such events will often lead to final states with leptons in jets. If we wish to use lepton plus jet events as a signature for new physics we must understand the background due to heavy quark production and decay. New results were reported at this conference on the number of D^* per jet by the UA1 collaboration[18] and by the CDF collaboration[19].

The number of $Q\bar{Q}$ pairs per gluon jet is calculable[20]. A gluon decaying into a heavy quark pair must have a virtuality $k^2 > 4m^2$. Perturbative methods should be applicable for a sufficiently heavy quark. The calculation has two parts. Firstly one has to calculate $n_g(E^2, k^2)$, the number of gluons of off-shellness k^2 inside the original gluon with off-shellness E^2 . Secondly, one needs the transition probability of a gluon with off-shellness k^2 to decay to a pair of heavy quarks.

The number of gluons of mass squared k^2 inside a jet of virtuality E^2 is given by,

$$n_g(E^2, k^2) = \left[\frac{\ln(E^2/\Lambda^2)}{\ln(k^2/\Lambda^2)} \right]^a \frac{\exp \sqrt{[(2N_c/\pi b) \ln(E^2/\Lambda^2)]}}{\exp \sqrt{[(2N_c/\pi b) \ln(k^2/\Lambda^2)]}} \quad (1.6)$$

where

$$a = -\frac{1}{4} \left[1 + \frac{2n_f}{3\pi b} \left(1 - \frac{V}{2N_c^2} \right) \right], \quad V = 8, N_c = 3, b = \frac{11N_c - 2n_f}{12\pi} \quad (1.7)$$

and b is the first order coefficient in the expansion of the β function. The correct calculation of the growth of the gluon multiplicity, Eq. (1.6), requires the imposition of the angular ordering constraint which takes into account the coherence of the emitted soft gluons.

$R_{Q\bar{Q}}$ is the number of $Q\bar{Q}$ pairs per gluon jet. The final result for the number of heavy quark pairs per gluon jet is[20],

$$R_{Q\bar{Q}} = \frac{1}{6\pi} \int_{4m^2}^{E^2} \frac{dk^2}{k^2} \alpha_S(k^2) \left[1 + \frac{2m^2}{k^2} \right] \sqrt{1 - \frac{4m^2}{k^2}} n_g(E^2, k^2) \quad (1.8)$$

The predicted number of charm quark pairs per jet is plotted in Fig. 6 using a value of $\Lambda^{(3)} = 300$ MeV and three values of the charm quark mass. For comparison the number of bottom quarks per jet with $\Lambda^{(4)} = 260$ MeV is also shown plotted in Fig. 6. The data point shows the number of D^* per jet as measured by the UA1 collaboration[18] and by the CDF collaboration[19]. In order compare these numbers with the $c\bar{c}$ pair rates shown plotted in Fig. 6, a model of the relative rates of D and D^* production is needed. For example, if all spin states are produced equally one would expect the charged D^* rate to be 75% of the total D production rate. The points in Fig. 6 need to be corrected upward for unobserved modes before they can be compared with the curves for the total $c\bar{c}$ pair rate.

2. Jet Physics

2.1 Inclusive spectra and compositeness limit.

Fig. 7 shows a comparison of the jet E_T distribution obtained at the ISR[21], the CERN collider [22] and the Tevatron[23]. The data are in good agreement with the predictions of perturbative QCD over many orders of magnitude. The theoretical

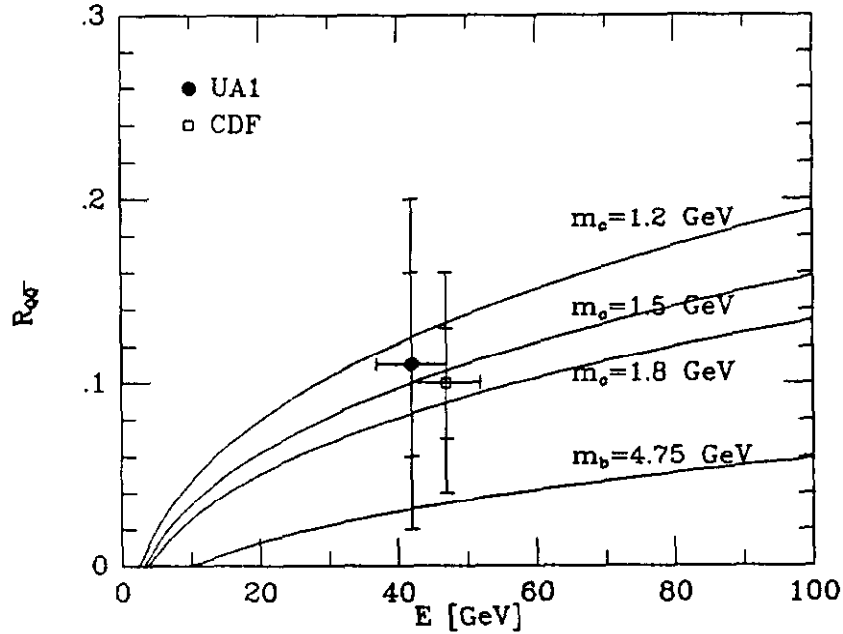


Figure 6: Heavy quarks in jets compared with UA1 and CDF data.

curves are lowest order and vary due to the choice of scale in the coupling constant and the parton distribution functions. These variations are too small to be visible on a logarithmic plot. In addition the experimental errors due to the overall scale uncertainty are large.

If quarks are composite the couplings between gauge bosons and fermions develop form factors. Deviations from point-like behaviour should be observed as the compositeness scale Λ^* is approached. Due to interference effects the existence of quark substructure should be apparent well below the energy scale associated with the binding of the constituents. Because identical quarks must share common constituents, flavour diagonal contact interactions are necessarily induced. For example, in models in which both chiral components of the quark field q are composite, the contact terms are,

$$L_{\text{int}} = \frac{g_m^2}{2\Lambda^{*2}} \left[\eta_{LL} \bar{q}_L \gamma^\mu q_L \bar{q}_L \gamma_\mu q_L + \eta_{RR} \bar{q}_R \gamma^\mu q_R \bar{q}_R \gamma_\mu q_R + 2\eta_{LR} \bar{q}_L \gamma^\mu q_L \bar{q}_R \gamma_\mu q_R \right] \quad (2.1)$$

These operators, which are low energy manifestations of the constituent interchange process, can be used to set a limit on the scale at which quark substructure manifests itself[24]. If Λ^* is larger than the scale of electroweak symmetry breaking, the

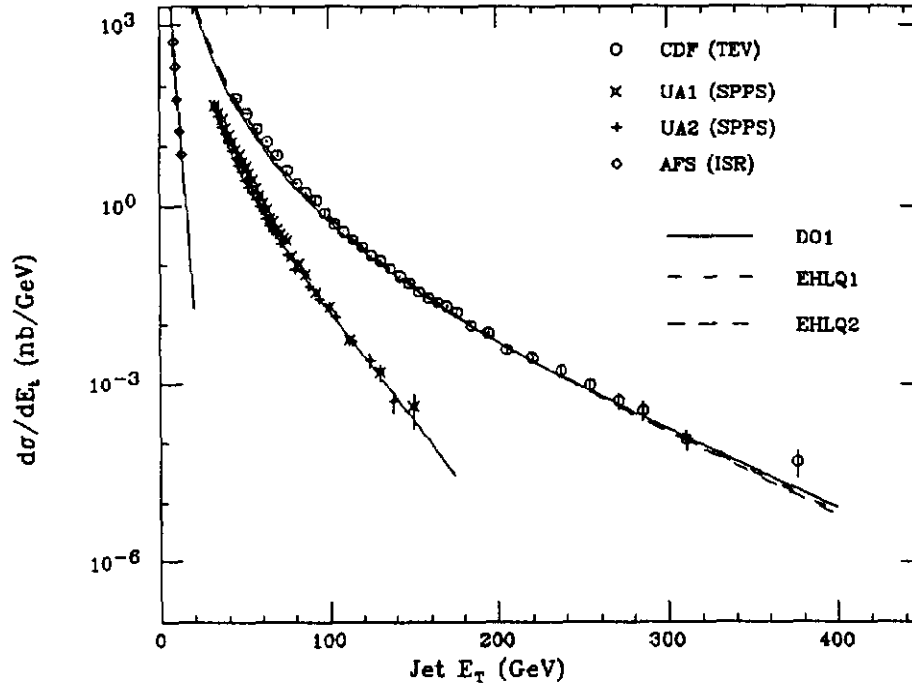


Figure 7: Comparison of inclusive jet data.

left-handed and right-handed fields are distinct species and the induced contact interaction should not conserve parity. For simplicity, the form of the contact term is taken to be,

$$L_{int} = \frac{4\pi}{\Lambda^{*2}} \bar{q}_L \gamma^\mu q_L \bar{q}_L \gamma_\mu q_L. \quad (2.2)$$

This corresponds to the choice $g_m^2/(4\pi) = 1$ for the strength of new metacolor interaction. This contact interaction gives rise to interference terms in the cross section of order $s/(\Lambda^{*2}\alpha_S)$ relative to the standard point-like interactions. Fig. 8 shows the effect of compositeness on the jet-jet invariant mass distribution. Bertolucci[23] has presented data on $d\sigma/dE_T$ normalised to $E_T < 150$ GeV and set the following limit on the compositeness scale.

$$\Lambda^* > 0.95 \text{ TeV at } 90 \% \text{ confidence level.} \quad (2.3)$$

This compositeness test is becoming quite stringent. In compositeness models in which the electroweak symmetry breaking is due to a condensate of preonic fields which also generate the quark masses, the scale Λ^* is expected to be of order $\sqrt{(v^3/m)}$ where $v \approx 250$ GeV is the scale of electroweak symmetry breaking. This compos-

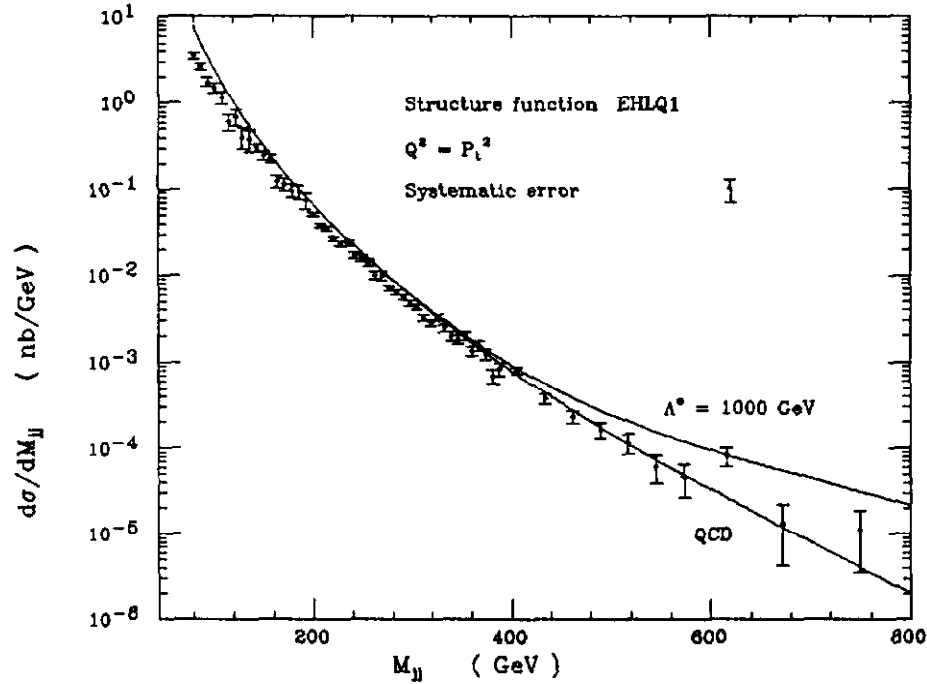


Figure 8: Compositeness limit.

iteness limit only applies to quarks and in no way constrains the scale of electron compositeness.

2.2 Higher order corrections to jet cross-sections.

Recently two groups[25,26] have used the higher order corrections to the two-to-two scattering matrix elements[27] to calculate jet cross-sections. Two important features emerge from this work. Firstly, the dependence on the scale μ at which the coupling constant and the parton distributions are evaluated is reduced after the inclusion of the higher order terms. Secondly, the cross section depends on the size of the cone used in the definition of the jet. In fact, the dependence on the cone size is a testable prediction of the theory. The presently published theoretical results on the jet cross sections are for a limited number of sub-processes and are therefore partial results. Full results should be forthcoming soon.

2.3 Observation of the hadronic decays of the vector bosons

The UA2 collaboration[28] have made a detailed study of the jet-jet invariant mass distribution and have found evidence for the hadronic decays of the vector bosons. This analysis is an extension of earlier work[29] by the UA2 collaboration. The motivation for this work is to check standard model predictions and to provide a test case for jet spectroscopy at hadron colliders. The experimental challenge of this analysis is formidable, since it requires an understanding of the QCD background and control on the scale and resolution of the mass measurement.

The UA2 collaboration have measured the jet-jet invariant mass distribution and attempted a fit to the data with the following three functional forms,

$$\frac{d\sigma}{dm_{jj}} = m_{jj}^{\alpha} \text{ or } m_{jj}^{\alpha} e^{-\beta m} \text{ or } m_{jj}^{\alpha} e^{-\beta m} e^{-\gamma m^2} \quad (2.4)$$

The fits are found to be rather poor. They therefore refit the data excluding a mass region Δm with a central value $\langle m \rangle$. The best fit is obtained with the choices $\Delta m = 30$ GeV and $\langle m \rangle = 85$ GeV. Note that this region has been selected in an unbiased way without any assumption on the line shape.

To proceed further the UA2 collaboration now make specific assumptions about the line shape.

$$M_Z/M_W = 1.14, \quad \frac{\Gamma(Z \rightarrow q\bar{q})}{\Gamma(W \rightarrow q\bar{q})} = 0.43 \quad (2.5)$$

The fit to the data is shown in Fig. 9. They obtain a five standard deviation peak

$$5620 \pm 1130 \text{ events, } m_W = 78.9 \pm 1.5 \text{ GeV} \quad (2.6)$$

Monte carlo studies using the measured vector-boson cross sections from UA2, Eq. (3.4), give an expectation of 4250 ± 150 events. Note however that the interference effects between QCD and electroweak processes can substantially modify both the shape of the invariant mass distribution and the event rate[30]. They must therefore be included if the W, Z rates are to be determined from the measured distribution.

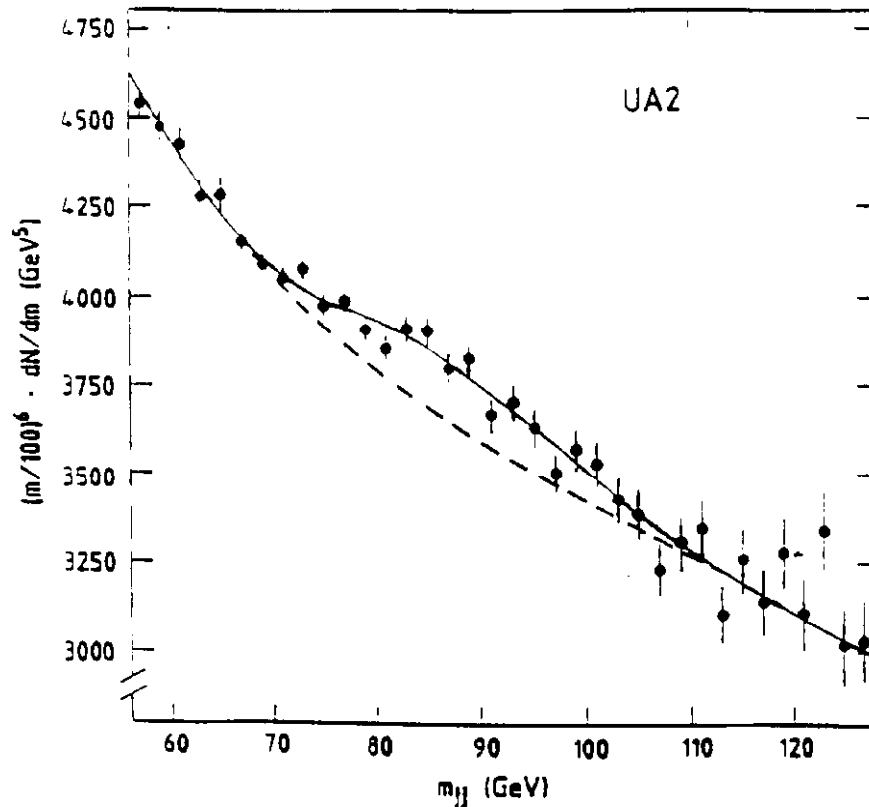


Figure 9: Evidence for the hadronic decays of the W and Z .

3. Vector boson production.

3.1 Lepton pair production.

The cross-section for the continuum production of muon pairs has been presented by the UA1 collaboration [31]. The result in the region above the upsilon is

$$\sigma(M_{\mu\mu} > 11 \text{ GeV}/c^2) = 0.24 \pm 0.04 \text{ (stat)} \pm 0.05 \text{ (sys) nb.} \quad (3.1)$$

Within the large errors this is in agreement with the production rate shown in Fig. 10. UA1 have also presented results on upsilon production[31] which are in agreement with earlier measurements,

$$\sigma(p\bar{p} \rightarrow \Upsilon, \Upsilon'\Upsilon'')B(\Upsilon, \Upsilon'\Upsilon'' \rightarrow \mu^+\mu^-) = 0.75 \pm 0.10 \text{ (stat)} \pm 0.20 \text{ (sys) nb.} \quad (3.2)$$

The cross section is an order of magnitude bigger than found in pp collisions at the ISR. This is in accordance with expectations from the gluon fusion model.

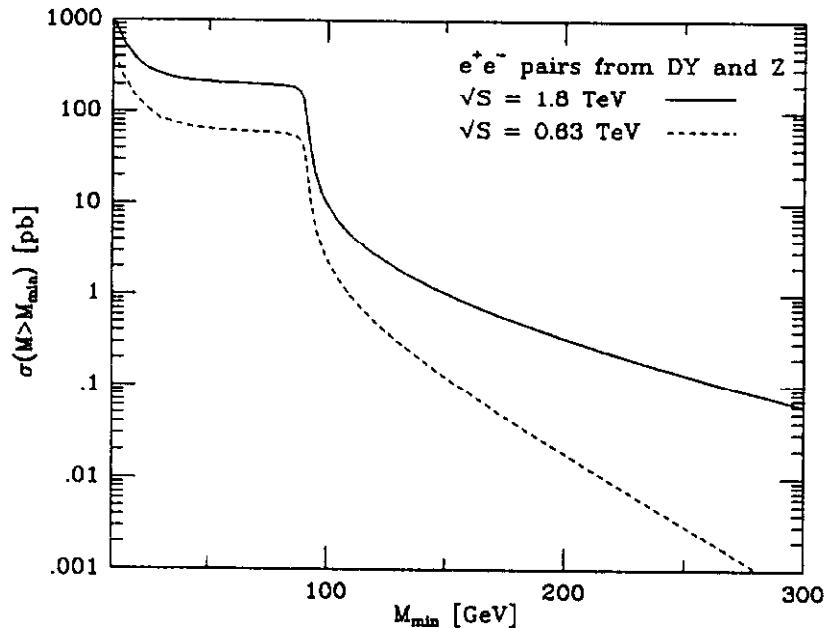


Figure 10: Predicted total rate for Drell-Yan pairs.

By examination of a sample of high mass unlike sign lepton pairs a lower limit can be set on the mass of a possible new vector boson. In general, bounds on the mass can be set only after assumptions about the couplings to quarks and leptons have been made. Assuming the new vector boson, Z' , has the same couplings as the Z of the standard model, the UA2 collaboration obtain $M_{Z'} > 216$ GeV at 90% confidence level[32]. It is amusing to note that the UA2 collaboration have one event with $M = 279$ GeV. They estimate that the number of electron pairs with mass greater than 200 GeV in 7.8 pb^{-1} of data from standard model sources should be 0.035. A similar estimate can be obtained from Fig. 10. At the Tevatron the cross-section for the production of lepton pairs with a mass greater than 200 GeV and standard model couplings is more than ten times bigger than at CERN. No limit on the mass of a Z' boson has been presented by CDF. From Fig. 10 one can anticipate that with their present data sample the CDF collaboration is sensitive to a Z' with standard model couplings and a mass of at least 300 GeV.

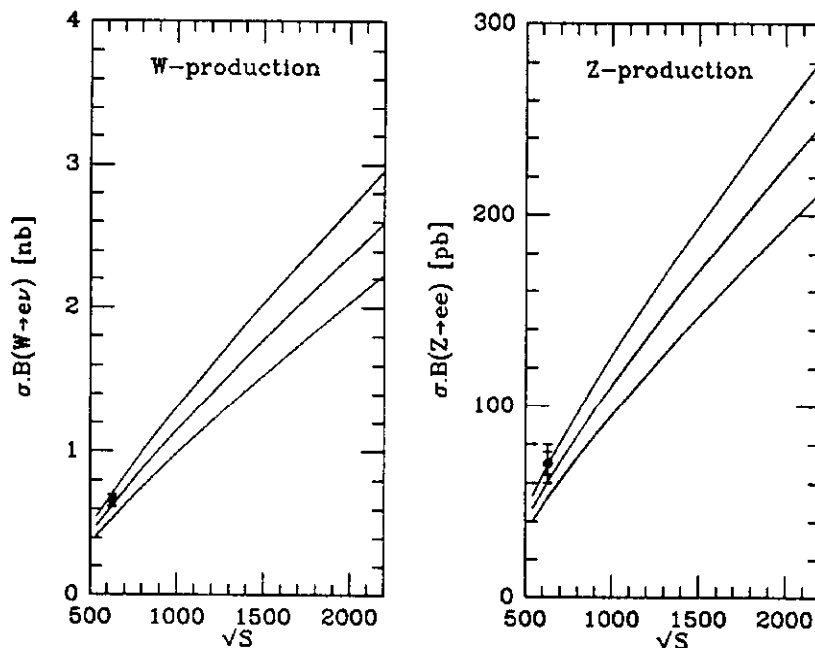


Figure 11: Predicted total cross section for W and Z.

3.2 Production properties of W's and Z's.

The cross-sections for vector boson production are determined by the parameters of the standard model and the parton distribution functions. The three quantities α , G_F and M_Z are well measured and hence will serve as the fundamental parameters. In the standard model M_W can be calculated from these parameters, if the mass of the top quark is known. Since the mass of the top quark is not yet known, we consider M_W also to be a free parameter to be determined by experiment. We use the values

$$\alpha(M_Z) = \frac{1}{128.8}, \quad G_F = 1.166 \times 10^{-5} \text{ GeV}^{-2}, \quad M_Z = 91.17 \text{ GeV}, \quad M_W = 80.3 \text{ GeV.} \quad (3.3)$$

which are derived from M_Z as determined by Mark II and $M_Z - M_W$ as determined by CDF. In the standard model these values imply a top quark of mass about 150 GeV (with large errors). The branching ratios to leptonic final states are calculated assuming that neither the W nor the Z can decay into the top quark. Table 2 shows the cross sections calculated in $O(\alpha_S)$ using the parton distributions of DFLM[33] and the value of $\Lambda^{(5)} = 170 \text{ MeV}$. The order $O(\alpha_S)$ terms contribute about 25% to the total. The theoretical error on these numbers shown in Fig. 11. The theoretical

	σ^W [nb]	$\sigma^W \cdot B$ [pb]	σ^Z [nb]	$\sigma^Z \cdot B$ [pb]
$\sqrt{S} = 630$ GeV, $\Lambda = 170$ MeV	5.78	626	1.80	61
$\sqrt{S} = 1800$ GeV, $\Lambda = 170$ MeV	19.8	2146	6.07	203

Table 2: Central values of theoretical cross sections for W and Z production.

errors are estimated to be $\pm 10\%$ from corrections of order α_s^2 and higher, $\pm 3\%$ from structure function uncertainties and $\pm 1\%$ from the uncertainty in the mass of the W . The most recent results for the vector boson cross sections at $\sqrt{S} = 630$ GeV from UA2[34] are in good agreement with theory.

$$\sigma^W B = 660 \pm 15(\text{stat}) \pm 37(\text{sys}) \text{ pb}, \quad \sigma^Z B = 70 \pm 6(\text{stat}) \pm 4(\text{sys}) \text{ pb} \quad (3.4)$$

The production of W 's in association with jets is important because it represents one of the principal sources of background to top searches in the electron plus jets channel. CDF results on the p_T of the W have been reported by Kamon[36]. The inclusive p_T distribution is a good place to check the production dynamics of vector boson production, since the theory is well understood. A complete order $O(\alpha_s^2)$ calculation has been performed by two groups[37]. Fig. 12 shows the preliminary results on the W - p_T spectrum from the CDF collaboration. The data have been corrected for acceptance and efficiency, but not for the smearing due to the finite energy resolution. Also shown on the same plot are the predictions of Arnold and Reno for both the energy of the Tevatron and of the CERN collider. Results on the p_T of the W have also been reported by the UA2 collaboration[35]. They have performed a detailed study of the effects of detector resolution. They conclude that for small p_T there are uncertainties of similar size in the experiment and in the theory. At high p_T the effects of detector resolution introduce an uncertainty larger than the theoretical uncertainty. The fraction of the observed W 's above 25 GeV is found to be

$$\frac{\sigma^W(p_T > 25 \text{ GeV})}{\sigma^W} = 3.9 \pm 0.7 \pm 0.6\% \quad (3.5)$$

which is in agreement with the theoretical expectation[17] of between 3 and 6 %. Thus the UA2 collaboration find no evidence for physics beyond the standard model in W production at large p_T .

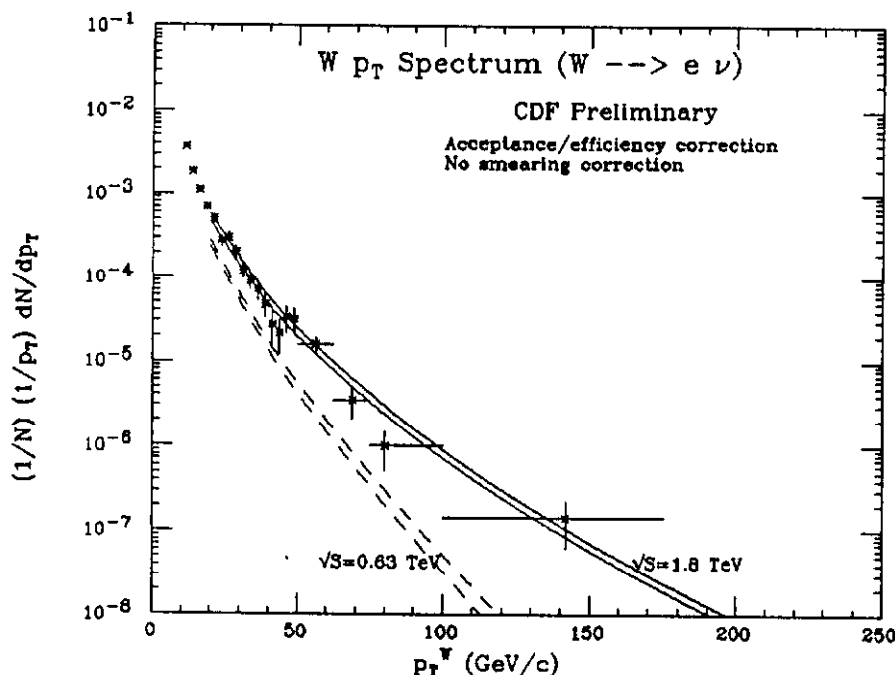


Figure 12: The transverse momentum distribution of W -bosons.

The UA1 collaboration[38] have reported preliminary results from their analysis of the 1988-1989 data sample. Before background subtraction they find two events with $p_T^W > 60$ GeV in a total sample of 489 ± 36 W candidates. These two events contain a W accompanied by two jets and are similar to the two events found in earlier runs[39]. The theoretical expectation[17] is that only about $0.3 \pm 0.09\%$ of the produced W 's should have $p_T^W > 60$ GeV at $\sqrt{S} = 0.63$ TeV. The corresponding figure at $\sqrt{S} = 1.8$ TeV is greater than 2%, so more copious production of this type of event would be expected at higher energy. Moreover the high p_T events are expected to contain predominantly one jet. Since CDF do not find an excess of two jet events at $p_T^W \approx 60$ GeV it appears unlikely that the UA1 events indicate the opening of a new physics threshold.

The p_T distribution of Z bosons is a good way to measure the strength of the QCD coupling because the transverse momentum of the vector boson is measured directly. At present the statistics are too low to make a good measurement. Preliminary results of the CDF collaboration are shown in Fig. 13 compared with the predictions of Arnold and Reno[37]. The effects of finite detector resolution have not been included.

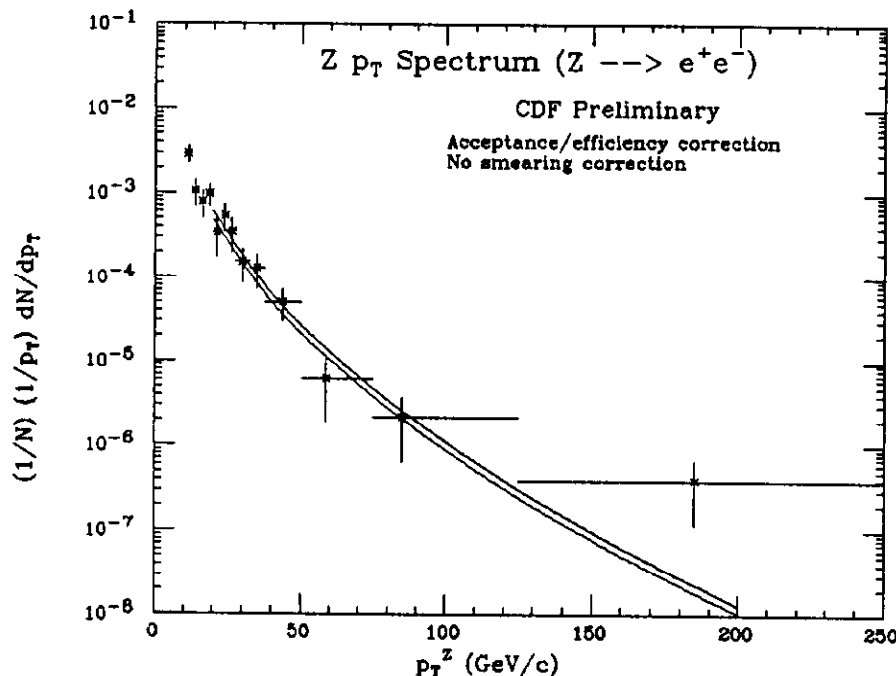


Figure 13: The transverse momentum distribution of Z -bosons.

3.3 The vector boson cross section ratio.

The ratio of the observed number of charged and neutral vector bosons has a long history associated with this conference. It was originally proposed by Cabibbo[40] at the Rome conference in 1983 as a method of counting the number of neutrinos, but it provides a precision test which is sensitive to several parameters of the standard model. The experimentally measured ratio for the observed leptonic decays can be expressed as follows,

$$R = \frac{\sigma(p\bar{p} \rightarrow W)B(W \rightarrow l\nu)}{\sigma(p\bar{p} \rightarrow Z)B(Z \rightarrow l+l^-)} = R_\sigma \cdot R_{BR}. \quad (3.6)$$

where R_{BR} is given by,

$$R_{BR} = \frac{B(W \rightarrow l\nu)}{B(Z \rightarrow l+l^-)} = \frac{\Gamma(W \rightarrow l\nu)}{\Gamma(W \rightarrow \text{all})} \frac{\Gamma(Z \rightarrow \text{all})}{\Gamma(Z \rightarrow l+l^-)} \quad (3.7)$$

The value of R_{BR} can be obtained from the measured R after inclusion of theoretical information on the ratio R_σ . Within the context of the standard model the value of R_{BR} depends on the mass of the top quark through the total W width, if the decay $W \rightarrow t\bar{b}$ is kinematically allowed. It also depends on the number of massless neutrino

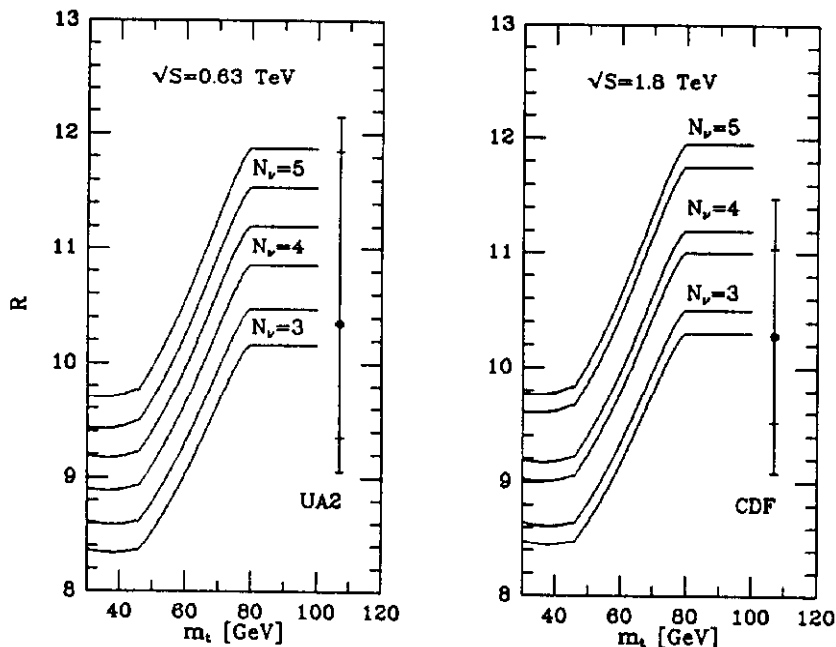


Figure 14: Comparison of data and theory for R ratio.

species through the total Z width. The presently quoted values[34,41] for this ratio are

$$\begin{aligned}
 R &= 10.35^{+1.5}_{-1.0}(\text{stat}) \pm 0.3(\text{syst}) : \text{UA2} \\
 R &= 10.3 \pm 0.8(\text{stat}) \pm 0.5(\text{syst}) : \text{CDF}
 \end{aligned}
 \tag{3.8}$$

These values are shown plotted in Fig. 14, compared with theoretical predictions from Martin, Roberts and Stirling[42].

The measurement of the ratio R will continue to be of interest through the next decade, although the particular features of the standard model which it tests will change as a consequence of results forthcoming from other experiments. The limits set on the top quark mass by R_{BR} have the advantage that they do not depend on any assumption about the semi-leptonic branching ratio of the top quark. Taking the width of the Z as measured by the e^+e^- colliders, SLC and LEP, $p\bar{p}$ colliders offer a unique opportunity to measure the width of the W . Using the values $R_r = 3.23 \pm 0.03$ and $\Gamma(Z) = 2.57 \pm 0.07$ GeV, the CDF collaboration find[41] $\Gamma(W) = 2.19 \pm 0.12$ GeV.

The measurements quoted above are statistically limited by the number of pro-

duced Z 's. An increase of the number of massless neutrinos from 3 to 4 increases the ratio R by 7%. Hence a measurement of the ratio R sensitive to fractions of a massless neutrino should be possible in the future. This should provide a nice confirmation of the results from e^+e^- annihilation.

The extraction of physics from the experimental value of R relies on an accurate estimate for the theoretical ratio R_σ and its errors. The dominant theoretical uncertainties in the R_σ ratio are the value of the weak mixing angle, θ_W , and the values of the parton distribution functions. The sensitivity to the parton distributions enters especially through the distribution of charm quarks and the ratio of the valence distributions of up and down quarks. At CERN energies the W and Z cross sections are particularly sensitive to u_v/d_v . At Tevatron energies there is a sensitivity to the charm distribution function which appears linearly in the W cross section, but quadratically in the Z cross section. There is also some sensitivity to the exact value of the masses of the W and the Z . This is related to the uncertainty in the weak mixing angle. The constraints placed on R_σ by measurements of the parton distributions are the subject of some theoretical debate. I refer the reader to the literature[42,43,44] for a complete discussion.

At Tevatron energies these uncertainties, which are individually of the order of a fraction of a percent, lead to total variations in the ratio R_σ which are of the order of 1%[42]. An estimate of the total uncertainty as evaluated by the authors of ref. [42] is indicated by the bands in Fig. 14. In view of the experimental errors it is clear that these ambiguities are not yet crucial. In the next decade as measurements improve these uncertainties will become more troubling. Note however that the argument can be turned around. If we can exclude the decay $W \rightarrow t\bar{b}$ and accept the standard model values for the vector boson decays with three massless neutrinos, the R measurement can be used to determine the parton distributions and weak mixing angle.

4. Vector boson properties

4.1 Vector boson masses

The reported values for the vector boson masses are shown in Table 3. For a detailed description of the mass measurements, I refer the reader to the contributed papers.

Experiment	Signal	Mass [GeV]
CDF-W[48]	$\approx 500 W \rightarrow \mu\nu$	$79.9 \pm 0.4(stat) \pm 0.6(sys)$
CDF-W[36]	1148 $W \rightarrow e\nu$	$80.0 \pm 0.2(stat) \pm 0.5(sys) \pm 0.3(scale)$
CDF-W	Combined	$80.0 \pm 0.6(stat + sys) \pm 0.2(scale)$
UA2-W[47]	1204 $W \rightarrow e\nu$	$80.79 \pm 0.31(stat) \pm 0.21(sys) \pm 0.81(scale)$
CDF-Z[46]	123 $Z \rightarrow \mu^+\mu^-$	$90.7 \pm 0.2(stat) \pm 0.4(sys)$
CDF-Z[46]	65 $Z \rightarrow e^+e^-$	$91.1 \pm 0.4(stat) \pm 0.3(sys)$
CDF-Z	Combined	$90.9 \pm 0.3(stat + sys) \pm 0.2(scale)$
UA2-Z[47]	49 $Z \rightarrow e^+e^-$	$90.2 \pm 0.6(stat) \pm 1.4(scale)$
MarkII-Z[49]	233 $e^+e^- \rightarrow Z$	$91.17 \pm 0.18(stat + sys)$

Table 3: Masses of the W and the Z

I shall comment further only on the efforts of the CDF collaboration to reduce the overall scale uncertainty in their mass measurement. The momentum of the observed decay products of the vector bosons can be derived from the curvature of the tracks, if the magnetic field is known. The magnetic field of the CDF solenoid has been mapped and is known with an uncertainty of $\pm 0.05\%$, leading to a momentum resolution of $\delta p/p^2 = 0.11\% (\text{GeV}/c)^{-1}$. The tracking mass scale can be checked by looking at the mass peaks of particles with known mass, but with generally softer tracks than the W and Z samples. The extrapolation to stiffer tracks should reduce the mass scale uncertainties. Thus, for example, the measured mass of the $J/\psi \rightarrow \mu^+\mu^-$ is 3.097 ± 0.001 in good agreement with the accepted values.

4.2 Precision tests of the Electro-weak theory

Ignoring the mass of the Higgs and the mass of the fermions the standard $SU(2) \times U(1)$ electroweak model contains three parameters. At the Lagrangian level these are the two gauge group couplings g and g' and the vacuum expectation value of the Higgs field v . These can be related to three measured parameters of electroweak interactions. Two physical parameters α and G_F are measured with great accuracy. After a determination of $\sin^2 \theta_W$, the standard model is completely specified (apart from the mass of the top quark and the Higgs). At tree graph level there are many equivalent definitions of $\sin^2 \theta_W$. Two of them are particularly appropriate for the

Experiment	s^2 (Marciano-Sirlin)
UA2-W and Z	0.220 ± 0.010
CDF-W and Z	0.225 ± 0.012

Table 4: Values of s^2 from vector boson masses

discussion of hadronic collider results.

$$\sin^2 \theta_W = 1 - \frac{M_W^2}{M_Z^2} \quad (4.1)$$

The weak mixing angle can also be determined from the effective four fermi coupling for Z boson exchange.

$$\mathcal{L} \propto (J_3^i - 2 \sin^2 \theta_W J_{\text{em}}^i)(J_3^j - 2 \sin^2 \theta_W J_{\text{em}}^j) \quad (4.2)$$

J_3 and J_{em} are the third component of the left-handed $SU(2)$ current and the electromagnetic current respectively. At one loop level these measures of $\sin^2 \theta_W$ are no longer equivalent. I shall therefore distinguish them and refer to the definition of Eq. (4.1) as s^2 and the definition of Eq. (4.2) as \bar{s}^2 . These differences, occurring first in one loop, are nominally of order α and hence too small to be observed in hadronic reactions, except if they are otherwise enhanced by a large factor. These large enhancements are of two types. The first type arise from large logarithms of the form $\alpha(\ln M_Z^2/m_f^2)$ where m_f is the mass of a light fermion. These logarithms are responsible for the difference in the values of the fine structure constant measured in the Thompson limit and at the mass of the Z [50].

$$\frac{1}{\alpha(M_Z)} = \frac{1}{\alpha}(1 - \delta\alpha), \quad \delta\alpha = 0.0601 \pm 0.0009 + \frac{40\alpha}{9\pi} \ln\left(\frac{m_Z}{91 \text{ GeV}}\right) \quad (4.3)$$

The second source of large corrections is from the non-decoupling of large masses, which is predominantly due to fermionic vacuum polarisation loops. This result is somewhat in contrast with the intuitive expectation that fluctuations in the vacuum involving heavy particles should have no effect on the theory at scales well below the heavy fermion mass. In spontaneous gauge theories not all heavy loops decouple. Fig. 15 (adapted from ref. [51]) shows the determination of the weak mixing angle from the new measurements of vector boson masses. The solid lines show the deter-

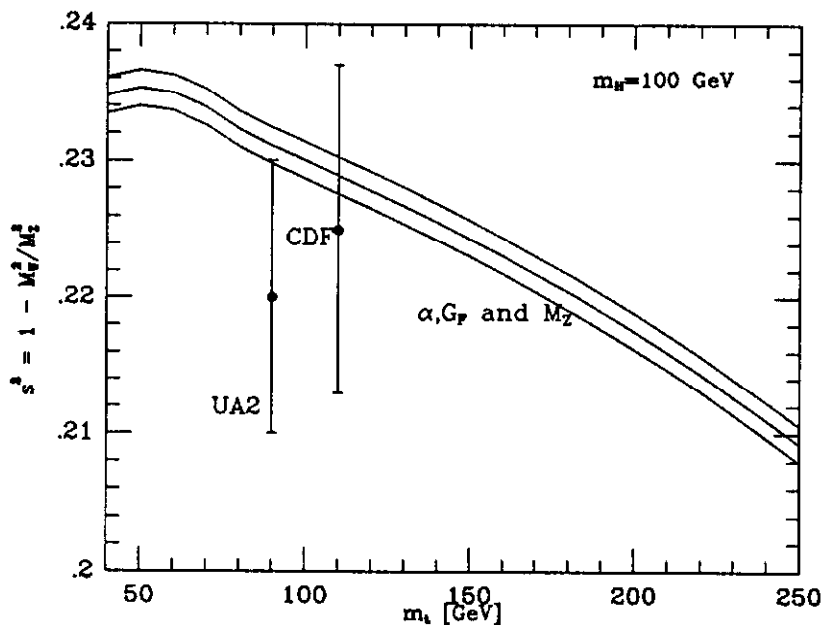


Figure 15: Weak mixing angle measurements as a function of top quark mass.

mination of s^2 , as defined in Eq. (4.1), from a measurement of M_Z . The three lines correspond to three values of the Z mass, (from top to bottom 90.7, 91.0 and 91.3 GeV). This determination is dependent on the top quark mass. This value of s^2 can be compared with other determinations of the weak mixing angle from low energy measurements. For a recent review I refer the reader to ref. [52]. The results on the neutral to charged current ratio R_ν in neutrino deep inelastic scattering are particularly important since this determination of s^2 is approximately independent of the value of the top quark mass. Comparison of the solid curve in Fig. 15 with the value derived from R_ν leads to an upper and lower bound on the top quark mass. The exact value of the bound depends primarily on the estimate of errors in the deep inelastic scattering measurement. These are mainly due to the application of the quark parton model in a kinematic region in which pre-asymptotic effects can have a considerable influence. From ref. [52] this bound on the top quark mass is estimated to be $m_t = 130 \pm 50$ GeV.

In view of the uncertainties of this analysis it is important to notice that measurements from colliders alone also lead to a upper bound on the mass of the top quark. In fact from Fig. 15 the combined value of s^2 from UA2 and CDF leads to an upper bound on the top quark mass in the range 250 to 300 GeV.

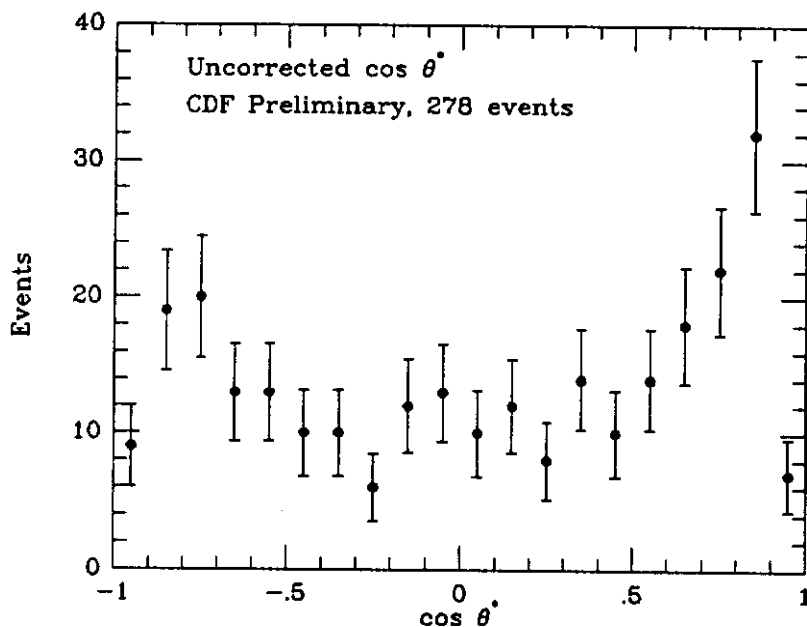


Figure 16: Forward-backward asymmetry on the Z

Other measurements of the weak mixing angle have been performed at hadronic colliders. The CDF collaboration has measured the forward backward asymmetry of electron-positron pairs at the Z pole[53]. The distribution of the sample of 278 events is shown in Fig. 16. The angle between the outgoing lepton and the incoming quark (or outgoing antilepton and incoming antiquark) in the dilepton centre of mass frame is denoted by θ^* . The asymmetry vanishes for a pure vector or pure axial vector coupling to the Z . From Eq. (4.2) the forward backward asymmetry is proportional to $1 - 4\bar{s}^2$ and hence provides a sensitive measure of \bar{s}^2 for $\bar{s}^2 \approx 0.23$. Using the effective factorised form Eq. (4.2), CDF derives a value of \bar{s}^2 .

$$\bar{s}^2 = 0.216 \pm 0.015(\text{stat}) \pm 0.010(\text{sys}) \quad (4.4)$$

Note that this value is without radiative corrections. An appreciable part of the systematic error is due to ignorance of the parton distributions, particularly the ratio u_v/d_v . The above value of \bar{s}^2 should be compared with the value $\bar{s}^2 = 0.24^{+0.05}_{-0.04}$ obtained previously by the UA1 collaboration[54].

For a large top mass \bar{s}^2 differs from s^2 because of the non-decoupling described

above. Retaining only the leading m_t^2 terms we have[55],

$$\bar{s}^2 = s^2 + \frac{3\alpha}{16\pi s^2} \frac{m_t^2}{M_Z^2} + O(\alpha) \approx s^2 + .01 \left(\frac{m_t}{200 \text{ GeV}} \right)^2. \quad (4.5)$$

5. Conclusions

There can be little doubt that the biggest change with respect to the $p\bar{p}$ conference of last year is the emergence of CDF as a major force. The combination of the higher energy of the Tevatron and an accumulated luminosity which is competitive with exposure obtained by the two major experiments at CERN, has allowed the CDF collaboration to reach, and in some cases surpass, the capabilities of the lower energy experiments.

One of the surprising results to emerge this year is the accuracy of the mass measurement of the Z boson. Of course the mass of the Z boson will most accurately be measured by e^+e^- machines when they begin to operate at full design luminosity. The result from hadronic colliders gives an idea of the precision which can be achieved in the measurement of the mass of the W . This latter measurement is the preserve of $p\bar{p}$ colliders until the startup of LEP II.

The more accurate value of the Z mass which has become available this year, in combination with the low energy measurements of the Weinberg angle, leads to a bound on the mass of the top quark in the region of 200 GeV. The preferred central value is 130 GeV. It is therefore within the range of the next Tevatron run which will have a luminosity of about 20 pb^{-1} . Collider measurements alone set a limit in the range $m_t < 250$ to 300 GeV.

The measurement of the cross-section ratio R for the production of W 's and Z 's, together with theoretical results on the production cross section and the W width lead to a limit on the number of neutrino species $n_\nu < 4.4$. Taking the Z width as known the ratio R can be used to measure the W width. This is currently possible only at hadron colliders.

It is very impressive to observe the speed with which physics results are derived from these complex experiments. Most of the results presented at this conference were obtained in the runs which finished only in the spring of 1989, a few months before the beginning of this conference. I look forward to seeing the final results.

Acknowledgement.

I would like to thank Giorgio Bellettini, Angelo Scribano and all the members of the local organising committee for their hospitality at Castiglione della Pescaia.

References

- 1) P. Nason, S. Dawson and R. K. Ellis, *Nucl. Phys.* **B303** (1988) 607 .
- 2) G. Altarelli *et al.*, *Nucl. Phys.* **B308** (1988) 724 .
- 3) A. Nisato, these proceedings.
- 4) S. Lammel, these proceedings.
- 5) D. Buskalic, these proceedings.
- 6) H. H. Williams, these proceedings;
F. Abe *et al.*, *Phys. Rev. Lett.* **64** (1990) 142 .
- 7) A. Barbaro-Galtieri, these proceedings;
F. Abe *et al.*, *Phys. Rev. Lett.* **64** (1990) 147 .
- 8) E. Low, these proceedings.
- 9) F. Porter, these proceedings.
- 10) W. A. Bardeen, C. T. Hill and M. Lindner, Fermilab-Pub-89/127-T, (1989).
- 11) S. Glashow and E. Jenkins, *Phys. Lett.* **196B** (1987) 233 .
- 12) M. Felcini, these proceedings.
- 13) S. Levegrün, these proceedings.
- 14) P. Nason, S. Dawson and R. K. Ellis, *Nucl. Phys.* **B327** (1989) 49 .
- 15) C. Albajar *et al.*, *Phys. Lett.* **B213** (1988) 405 .
- 16) N. Ellis, these proceedings.

- 17) G. Altarelli, R. K. Ellis and G. Martinelli, *Zeit. Phys.* **C27** (1985) 617 .
- 18) M. Ikeda, these proceedings.
- 19) R. Plunkett, these proceedings;
F. Abe *et al.*, *Phys. Rev. Lett.* **64** (1990) 348 .
- 20) A. H. Mueller and P. Nason, *Phys. Lett.* **157B** (1985) 226 .
- 21) T Akesson *et al.*, *Phys. Lett.* **123B** (1983) 133 .
- 22) J. Appel *et al.*, *Phys. Lett.* **160B** (1985) 349 ;
G. Arnison *et al.*, *Phys. Lett.* **172B** (1986) 461 .
- 23) S. Bertolucci, these proceedings;
M. Dell'Orso, these proceedings.
- 24) E. Eichten, K. Lane and M. Peskin, *Phys. Rev. Lett.* **50** (1983) 811 .
- 25) J.-P. Guillet, these proceedings.
- 26) S. D. Ellis, Z. Kunszt and D. Soper, *Phys. Rev. Lett.* **62** (1989) 726 .
- 27) R. K. Ellis and J. C. Sexton, *Nucl. Phys.* **B282** (1987) 642 .
- 28) K. Meier, these proceedings.
- 29) R. Ansari *et al.*, *Phys. Lett.* **186B** (1987) 452 .
- 30) U. Baur, E. W. N. Glover and A. D. Martin, CERN-TH-5523/89.
- 31) K. Ankoviak, these proceedings.
- 32) V. Vercesi, these proceedings.
- 33) M. Diemoz *et al.*, *Zeit. Phys.* **C39** (1988) 21 .
- 34) M. Lefebvre, these proceedings;
G. Blaylock, presentation at the 1990 Aspen Winter Physics conference.
- 35) D. Wood, these proceedings.
- 36) T. Kamon, these proceedings.

- 37) P. Arnold and M. H. Reno, *Nucl. Phys.* **B319** (1989) 37 and erratum Fermilab preprint PUB 89/59-T (1989);
P. Arnold, R. K. Ellis and M. H. Reno, *Phys. Rev.* **D40** (1989) 912 ;
R. Gonsalves, J. Pawlowski and C-F Wai, *Phys. Rev.* **D40** (1989) 2245 .
- 38) A. Böhrer, these proceedings.
- 39) C. Albajar *et al.*, *Phys. Lett.* **193B** (1987) 389 .
- 40) N. Cabibbo, Proceedings of the 3rd Topical Workshop on Proton-Antiproton Collider Physics, Rome 1983, CERN 83-04.
- 41) F. Abe *et al.*, *Phys. Rev. Lett.* **64** (1990) 152 .
- 42) A. D. Martin, R. Roberts and W. J. Stirling, *Mod. Phys. Lett.* **A12** (1989) 1135 ; *Phys. Lett.* **228B** (1989) 149 .
- 43) E. L. Berger *et al.*, *Phys. Rev.* **D40** (1989) 83 .
- 44) K. Hagiwara *et al.*, Madison preprint, MAD/PH/496 (1989).
- 45) W. Beenakker *et al.*, *Phys. Rev.* **D40** (1989) 54 .
- 46) F. Abe *et al.*, *Phys. Rev. Lett.* **63** (1989) 720 ;
T. Phillips, these proceedings.
- 47) K. Einsweiler, these proceedings;
G. Blaylock, presentation at the 1990 Aspen Winter Physics conference.
- 48) D. Smith, these proceedings.
- 49) Abrams *et al.*, *Phys. Rev. Lett.* **63** (1989) 724 .
- 50) M. Consoli, W. Hollik and F. Jegerlehner, in Z Physics at LEP, CERN report 89-08 (1989).
- 51) M. Peskin, Proceedings of the 17th SLAC Summer Institute (1989).
- 52) G. Altarelli, Proceedings of the XIV International Symposium on Lepton and Photon Interactions, (1989).
- 53) P. Hurst, these proceedings.

- 54) C. Albajar *et al.*, *Zeit. Phys.* **C44** (1989) 15 .
- 55) see, *e.g.*, W. Hollik, DESY preprint 88-188 (1988).